

# Novel Series and Shunt MEMS Switch Geometries for X-Band Applications

Jeremy B. Muldavin and Gabriel M. Rebeiz

Radiation Laboratory, Department of Electrical Engineering and Computer Science,  
University of Michigan, Ann Arbor, Michigan, 48109-2122, USA.  
[muldavin@engin.umich.edu](mailto:muldavin@engin.umich.edu), [rebeiz@umich.edu](mailto:rebeiz@umich.edu).

*Abstract*— In this paper, novel metal membrane series switches and inductively tuned shunt switches are presented. The series switch produces an isolation better than -30 dB at 5 GHz in the up-state and return loss less than -20 dB from DC to 20 GHz. The shunt switch geometry can be modified to specify the resonant frequency of the switch in the down-state. The shunt switch is modeled by an equivalent CLR circuit. The MEMS membrane height is 1.5-2.5  $\mu\text{m}$ , resulting in a pulldown voltage of 15-25 V. Application areas are in low-loss high-isolation communication and radar switches.

## I. INTRODUCTION

This paper focuses on the design, and implementation of coplanar waveguide (CPW) series and shunt MEMS switches for X-band high isolation applications. A novel metal membrane DC contact series switch and a novel shunt switch are presented and implemented in a series-shunt configuration. The fabrication of these switches is similar to that of a typical *air bridge*, making them low cost and easily integrable with traditional MMIC circuits. The switches are designed for X-band operation, but the designs can be easily extended to 40 GHz.

## II. METAL MEMBRANE SERIES SWITCH

A novel metal membrane MEMS series switch has been fabricated for DC to 20 GHz operation using a 50  $\Omega$  cpw line implementation (96,160,96  $\mu\text{m}$ ) on a high resistivity silicon substrate (Fig. 1). The

This work was supported by Jet Propulsion Lab, "System on a Chip" program.

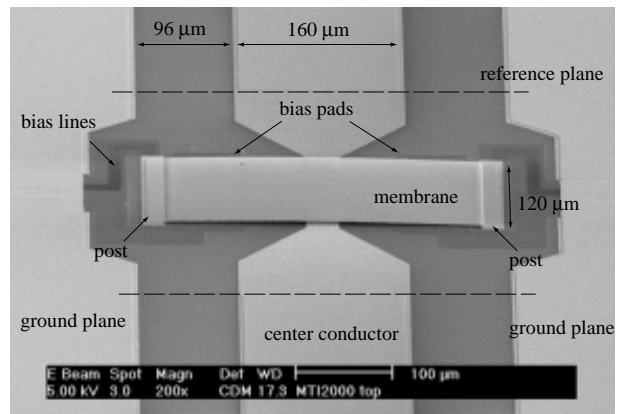


Fig. 1. SEM of a novel metal membrane MEMS series switch. The 6000  $\text{\AA}$  thick Au membrane is fixed at both ends and suspended 2.5  $\mu\text{m}$  above contact pads on either side of the 60  $\mu\text{m}$  center conductor gap.

switch is based on a 300  $\mu\text{m}$  long, 6000  $\text{\AA}$  thick *sputtered* gold membrane, fixed at each end and suspended 2.5  $\mu\text{m}$  above the gap in the center conductor. The metalization underneath the membrane is a 3000  $\text{\AA}$  thick Au. The width of the MEMS membrane is 120  $\mu\text{m}$  and the length is 300  $\mu\text{m}$ . The membrane is pulled down to the contact pads on either side of the center conductor gap when a voltage of 20-30 V is applied to the dielectric-covered bias pads under the membrane. The dielectric covered bias lines are made of 200  $\text{\AA}$  of evaporated NiCr with a resistance of 50  $\Omega/\text{square}$  and are fed under the ground planes to probe pads.

The measurements are based on an on-wafer TRL calibration [1] and are referenced to 40  $\mu\text{m}$  from the taper in the center conductor as shown in Figure 1. Figure 2 shows the measured performance of a 120  $\mu\text{m}$  wide series switch in the up and down-state. The isolation is better than -30 dB at 5 GHz in the down-state with a return loss is better than -20 dB

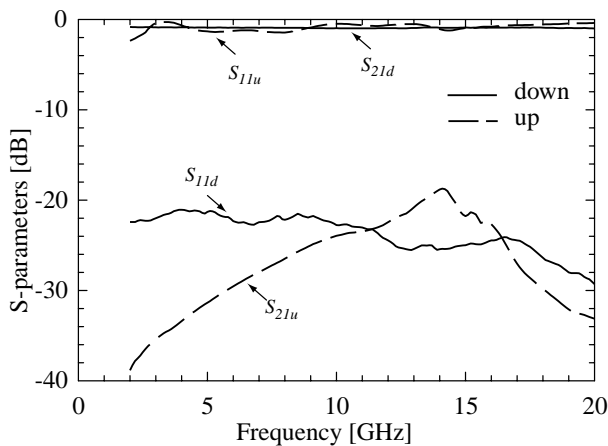


Fig. 2. Measured S-parameters of a metal membrane MEMS series switch in the up ( $S_{11u}$ ,  $S_{21u}$ ) and down-states ( $S_{11d}$ ,  $S_{21d}$ ).

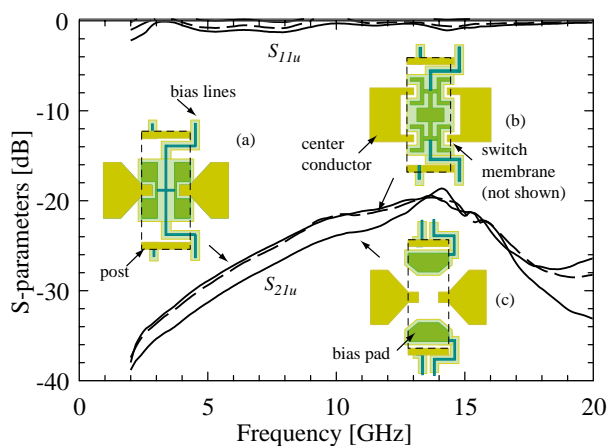


Fig. 3. Measured S-parameters of three different bias geometries for the metal membrane MEMS series switches in the up-state ( $S_{11u}$ ,  $S_{21u}$ ).

from DC to 20 GHz. The insertion loss for this series switch is around 0.5 dB from 2-20 GHz.

Figure 3 show the measured up-state isolation for three different bias pad geometries. Two of the geometries (a, b) place the bias pad within 10  $\mu\text{m}$  of the center conductor to improve the metal-to-metal contact when the bias voltage is applied. These contact geometries slightly decrease the up-state isolation as compared to the third bias geometry (c) where the bias pads are at least 40  $\mu\text{m}$  from the center conductors.

### III. NOVEL MEMS SHUNT SWITCH

A novel MEMS shunt capacitive switch has been fabricated using a 50  $\Omega$  cpw line implementation (96,160,96  $\mu\text{m}$ ) on a high-resistivity silicon substrate (Fig. 4). In this design, the center conductor is transitioned to a metal membrane suspended 2.5  $\mu\text{m}$  over a 5000  $\text{\AA}$  thick Au line connecting the two ground planes. Below the membrane, the ground-line is covered with 2100  $\text{\AA}$  thick silicon nitride. The width of the MEMS membrane is 100  $\mu\text{m}$  at the center and the length is 300  $\mu\text{m}$ . The membrane is pulled down to the ground-line when a voltage of 20-30 V is applied between the center conductor and the dielectric covered ground-line. This switch geometry is the complement of the standard MEMS shunt switch where the ground-line is a suspended membrane and the center conductor remains in contact with the substrate [2], [3], [4], [5].

As is the case for a standard MEMS shunt switch, for a given center conductor membrane, the area of the ground-line under the center conductor membrane determines the shunt capacitance of the switch and the width and length of the line leading to the ground plane determines the shunt inductance of the switch [6]. The inductance and capacitance resonate at  $\omega = 1/\sqrt{LC}$  with a quality factor of  $Q = \frac{1}{R}\sqrt{\frac{L}{C}}$ , where  $R$  is the resistance of the ground-line (Fig. 5). Figure 5 shows that a switch with  $W = 140 \mu\text{m}$ ,  $w_1 = 140 \mu\text{m}$ ,  $L_m = 226 \mu\text{m}$ , and  $w_2 = 30 \mu\text{m}$  has an equivalent inductance ( $L$ ) of 45 pH, a down-state capacitance ( $C_d$ ) of 6.5 pF, and a resistance ( $R$ ) of 0.15  $\Omega$ . The switch resonates at 9.3 GHz with a quality factor of 17. The transmission line geometry around the switch ( $L_m$ ,  $W$ ,  $w_1$ ,  $w_2$ ) can be modified to give different values of switch inductance and capacitance. In this way, the resonant frequency of the switch may be adjusted.

The measured and fitted down-state S-parameters for the MEMS shunt switch with  $C_d = 4.5$  pF and various ground-line geometries are shown in Fig. 6. As the line connecting the two ground planes becomes thinner or longer, the switch equivalent inductance increases, the resonant frequency decreases, and the  $Q$  of the resonance increases (bandwidth decreases). The isolation of a single shunt switch may therefore be increased by 10 to 20 dB at the expense of reduced bandwidth.

### IV. SERIES-SHUNT MEMS SWITCH

The series and shunt switch can be cascaded together to produce a high isolation switching element

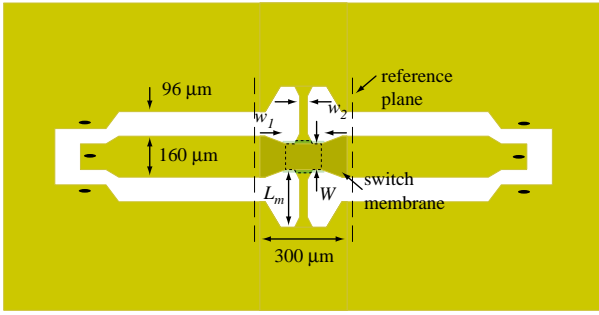


Fig. 4. Schematic of a novel MEMS shunt capacitive switch where the center conductor transitions to a membrane suspended over a dielectric-covered transmission line connecting the two ground planes.

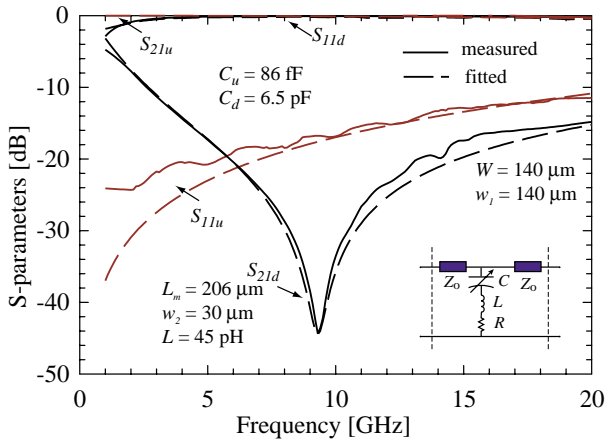


Fig. 5. Measured and fitted S-parameters of a novel MEMS shunt capacitive switch in the up-state and the down-state. The measured data is fitted using a simple shunt CLR model.

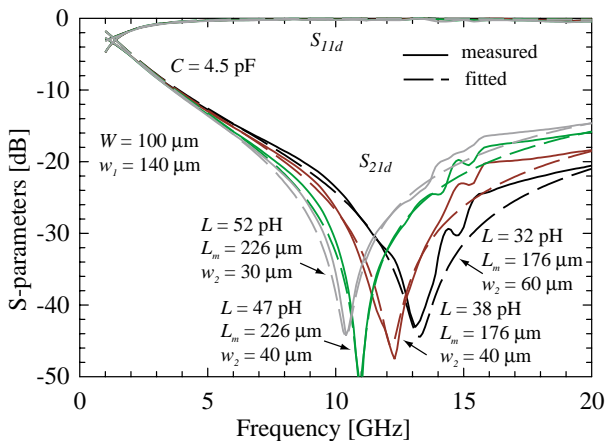


Fig. 6. Measured and fitted S-parameters of MEMS shunt capacitive switches with various ground-line geometries.

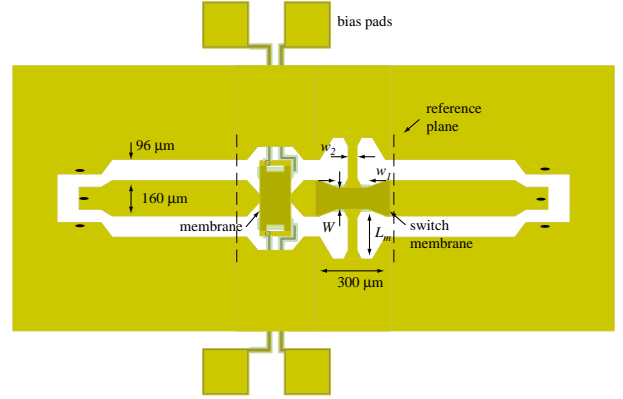


Fig. 7. Schematic of a series-shunt switch. The switch provides isolation when the series switch is in the up-state and the shunt switch is in the down-state. The switch provides low return loss when the series switch is in the down-state and the shunt switch is in the up-state.

with a wide bandwidth (Fig. 7). The switch provides high isolation when the series switch is in the up-state and the shunt switch is in the down-state. The switch provides low return loss when the series switch is in the down-state and the shunt switch is in the up-state. The fabrication processes for the two switches are compatible with each other as well as standard MMIC designs. Figure 8 shows the measured S-parameters for a series-shunt switch using the series switch in Fig. 1 and a shunt switch with  $L_m = 226 \mu\text{m}$ ,  $w_1 = 140 \mu\text{m}$ ,  $W = 100 \mu\text{m}$ , and  $w_2 = 40 \mu\text{m}$ . The measured isolation is improved from the single series switch. However, the isolation is much less than expected when compared to simulations of the cascaded S-parameters of the individual series and shunt switch measured S-parameters (Fig. 7). The decreased isolation may be the result of parasitic radiation and is currently under investigation. The latest results will be presented at the conference.

## REFERENCES

- [1] R. B. Marks, "A Multiline Method of Network Analyser Calibration," *IEEE Transactions on Microwave Theory and Techniques*, vol. 39, no. 7, pp. 1205–1215, July 1991.
- [2] N. S. Barker and G. M. Rebeiz, "Distributed MEMS true-time delay phase shifters and wideband switches," *IEEE Trans. on Microwave Theory and Techniques*, vol. 46, no. 11, pp. 1881–1890, Nov 1998.
- [3] N. S. Barker and G. M. Rebeiz, "Optimization of distributed MEMS phase shifters," in *1999 IEEE MTT-S Int. Microwave Symp. Dig.*, Anaheim, CA, June 1999, pp. 299–302.
- [4] C. Goldsmith, J. Randall, S. Eshelman, T. H. Lin, D. Den-nistor, S. Chen, and B. Norvell, "Characteristics of mi-

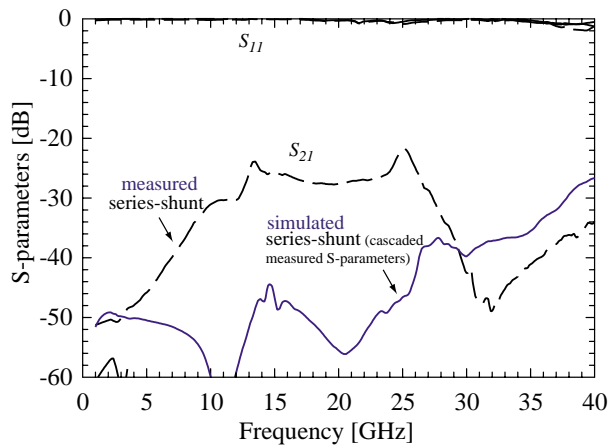


Fig. 8. Measured S-parameters for a series-shunt switch in the isolation state (series up, shunt down). For comparison, simulations using individual series and shunt switch S-parameters cascaded in Libra are presented. This simulation suggests that some form of parasitic radiation is limiting the isolation of the measured series-shunt switch.

cromachined switches at microwave frequencies,” in *1996 IEEE MTT-S Int. Microwave Symp. Dig.*, San Francisco, CA, June 1996, pp. 1141–1144.

- [5] C. Goldsmith, T. H. Lin, B. Powers, W. R. Wu, and B. Norvell, “Micromechanical membrane switches for microwave applications,” in *1995 IEEE MTT-S Int. Microwave Symp. Dig.*, Orlando, FL, June 1995, pp. 91–94.
- [6] J. B. Muldavin and G. M. Rebeiz, “Design and modeling of high-isolation MEMS switches,” in *1999 IEEE MTT-S Int. Microwave Symp. Dig.*, Anaheim, CA, June 1999, pp. 1151–1154.